

CCR4 expression on host T cells is a driver for alloreactive responses and lung rejection

Vyacheslav Palchevskiy, ... , David G. Brooks, John A. Belperio

JCI Insight. 2019. <https://doi.org/10.1172/jci.insight.121782>.

Research [In-Press Preview](#) [Immunology](#) [Transplantation](#)

Despite current immunosuppressive strategies, long-term lung transplant outcomes remain poor due to rapid allogeneic responses. Using a stringent mouse model of allo-airway transplantation, we identify the CCR4-ligand axis as a central node driving secondary lymphoid tissue homing and activation of the allogeneic T cells that prevent long-term allograft survival. CCR4 deficiency on transplant recipient T cells diminishes allograft injury and when combined with CTLA4-Ig leads to an unprecedented long-term lung allograft accommodation. Thus, we identify CCR4-ligand interactions as a central mechanism driving allogeneic transplant rejection and suggest it as a potential target to enhance long-term lung transplant survival.

Find the latest version:

<https://jci.me/121782/pdf>



Title

CCR4 Expression on Host T cells is a Driver for Alloreactive Responses and Lung Rejection

Authors

Vyacheslav Palchevskiy¹, Ying Ying Xue¹, Rita Kern¹, Stephen S. Weigt¹, Aric L. Gregson¹, Sophie X. Song¹, Michael C. Fishbein¹, Cory M. Hogaboam², David M. Sayah¹, Joseph P. Lynch, III¹, Michael P. Keane³, David G. Brooks⁴ and John A. Belperio^{1*}.

Affiliations

¹Department of Medicine, David Geffen School of Medicine, University of California, Los Angeles, California, USA.

²Pulmonary & Critical Care Medicine, Cedars-Sinai Medical Center, Los Angeles, California, USA.

³UCD School of Medicine, Respiratory Medicine, St Vincent's University Hospital, Dublin, Ireland.

⁴Princess Margaret Cancer Center, University Health Network and Department of Immunology, University of Toronto, Toronto, ON, M5G 2M9 Canada.

*Corresponding author.

John A. Belperio MD

UCLA, David Geffen School of Medicine

Division of Pulmonary & Critical Care Medicine

650 Charles E. Young Dr S

Center for the Health Sciences, 52-243

Los Angeles, CA 90095

Email: JBelperio@mednet.ucla.edu

(310) 794-1992

Conflict of Interest

The authors have declared no conflict of interest exists.

Abstract

Despite current immunosuppressive strategies, long-term lung transplant outcomes remain poor due to rapid allogenic responses. Using a stringent mouse model of allo-airway transplantation, we identify the CCR4-ligand axis as a central node driving secondary lymphoid tissue homing and activation of the allogeneic T cells that prevent long-term allograft survival. CCR4 deficiency on transplant recipient T cells diminishes allograft injury and when combined with CTLA4-Ig leads to an unprecedented long-term lung allograft accommodation. Thus, we identify CCR4-ligand interactions as a central mechanism driving allogeneic transplant rejection and suggest it as a potential target to enhance long-term lung transplant survival.

Introduction

Lung transplants have among the worst overall long-term clinical outcomes with a 5 year survival of less than 55% (1). This is particularly concerning when compared to other solid organ transplants such as liver, kidney and heart that have 5 year survival rates of at least 70% (1-6). Lung transplant recipients also have much higher rates of rejection, the main risk factor for limited lung allograft survival (7-15). Rejection is classically considered a consequence of an immune response to donor alloantigens that results in allograft dysfunction (7-15). However, many of the molecular factors involved in the initiation of the alloresponse that leads to rejection remain largely unknown.

Rejection of solid organs involves alloresponsive lymphocytes and delayed type hypersensitivity (DTH). The alloresponse begins with the homing of recipient-derived naïve T cells (T_n) to secondary lymphoid tissues (SLT). Once inside SLT, T_n traffic intranodally to antigen presenting cells (APC) and this interaction generates allo-specific T cells in a process called allopriming. The allo-specific lymphocytes egress from the SLT, traffic to the transplanted organ and release cytotoxic mediators that directly injure the allograft. The alloreactive lymphocytes also initiate a DTH response that directs waves of activated leukocytes into the allograft further destroying the injured graft, ultimately leading to graft failure.

Many, but not all studies have suggested that non-transplant T cell priming within lymph nodes is independent of chemokines due to the efficient scanning capabilities between T_n and APC (16-27). This has led to a paucity of information involving the role of chemokines orchestrating allopriming. Interestingly, we observed high levels of the chemokines CCL17 and CCL22 in draining lymph nodes following allograft transplantation using a stringent mouse model of heterotopically placed airway grafts. Considering that the receptor for these chemokines, CCR4 has been described on T_n cells (28-30), we sought to determine whether the CCR4-ligand biological axis mediates the alloreactive

immune response following transplantation. Herein, we demonstrate that CCR4 expression on host derived T cells is critical for their homing to draining lymph nodes and intranodal activation, which drives the alloreactive response involved in transplant rejection. CCR4 deletion on T cells reduced airway allograft rejection. Interestingly, CCR4 deficiency in combination with a short peri-operative course of CTLA4-Ig enabled an unprecedented long-term allograft survival over 125 days compared to approximately one month when CTLA4-Ig was administered to CCR4^{+/+} recipients. This remarkable observation was corroborated in the fully vascularized murine left single lung transplant model. Thus, we identify the CCR4-ligand axis as a critical checkpoint in driving the allogeneic response leading to transplant rejection and indicate a new target for a therapeutic intervention to maintain long-term organ survival.

Results

Draining SLT has increased CCL17 and CCL22 expression during allograft rejection

Previous studies have demonstrated that Tn cells express the CCR4 receptor while mononuclear phagocytes and APC can be a rich source for its ligands CCL17 and CCL22 (28-30). We used the fully mismatched heterotopic tracheal transplant model of airway allograft rejection to explore the role of CCR4-ligands interaction in allograft rejection. BALB/c airways were transplanted subcutaneously into C57BL/6 recipients (allografts) and C57BL/6 airways into C57BL/6 recipients (isografts). This model of rejection is a highly reproducible and over time results in pathology that is representative of human acute rejection and chronic lung allograft dysfunction (31-35). A kinetic evaluation of the CCR4 ligands from whole draining SLT (axillary and brachial nodes) homogenates using Luminex technology demonstrates marked elevations of both CCL17 and CCL22 protein concentrations at days 7 and 14 from allografts, as compared to isografts (Figure 1A). We also determined the cellular sources of these chemokines by performing immunohistochemical (IHC) analysis on allograft draining SLT (n=4) at day 7 post-transplant. Morphometrically, we observed that CCL17 is predominately expressed from high endothelial venules (HEV) in the paracortical areas (Figure 1B). CCL22 protein localized predominately to the paracortical and subcapsular sinus mononuclear phagocytes (Figure 1C). These chemokine expression patterns are poised to work together in bringing Tn to SLT as well as allow them to traffic within the node to APC.

The inhibition of CCR4 interactions with its ligands profoundly attenuates allograft rejection

The increased levels of CCL17 and CCL22 in SLT from allograft recipients suggested that perturbing the CCR4-ligand axis could inhibit allograft injury. To test this, BALB/c airways were transplanted into C57BL/6 CCR4^{-/-} or CCR4^{+/+} recipients and the allografts were harvested at

multiple time points for histopathological rejection scoring based on leukocyte infiltration, epithelial injury, matrix deposition and fibro-obliteration (32, 33, 36). BALB/c donor airways prior to transplant demonstrate minimal inflammation, normal epithelium and no matrix deposition or fibrosis (Figure 2A). CCR4^{-/-} recipients had profound reductions in rejection, as compared to CCR4^{+/+} recipients at days 7, 14, 21 and 28 (Figure 2, A and B, and Supplemental Figure 1A). More specifically, the allografts from the CCR4^{+/+} recipients developed marked leukocyte infiltration with epithelial cell injury at day 7, persistent inflammation with partially denuded epithelium and matrix deposition at day 14 and a denuded epithelium with invading fibroblasts obstructing the allograft airways at days 21 and 28. In contrast, the airway allografts from the CCR4^{-/-} recipient mice had mild to moderate inflammation with a preserved epithelium and no significant matrix deposition or fibroblast obliteration throughout the 28-day time course (Figure 2, A and B, and Supplemental Figure 1A). Interestingly, a recent study insinuates that CCR4 is required for T cell development, therefore the CCR4^{-/-} recipient mice could have an altered T cell repertoire (37), which could be responsible for the reduction in allograft rejection. Thus, we performed confirmatory studies involving donor BALB/c airways transplanted into C57BL/6 recipients treated with either a CCR4 antagonist or an appropriate control. More specifically, recipient mice were treated with the small molecule CCR4 antagonist C 021 dihydrochloride (Tocris) at 50 mg/kg versus appropriate control administered intraperitoneally every day beginning at day -1 until allograft harvesting for rejection scoring at day 14 (38). The CCR4 antagonist led to similar reductions in rejection scores as the CCR4^{-/-} recipients when compared to appropriate controls (Figure 2, C and D). These results suggest that the CCR4^{-/-} recipients ability to attenuate allograft rejection is not due to altered microbiota or possibly altered CCR4^{-/-} T cell repertoire.

CCR4 ligands have been implicated in the recruitment of APC to draining SLT (39). Furthermore, it has been established that donor-derived APC can migrate from the transplanted organ to the recipient SLT where they are involved in the initiation of rejection (40). To test the role of CCR4 on donor APC, we transplanted donor airways from C57BL/6 CCR4^{-/-} mice into BALB/c recipients so that only the donor-derived cells would lack CCR4. However, in this situation we did not observe any alterations in allograft rejection scores at days 7, 14 or 21; and both CCR4^{+/+} and CCR4^{-/-} donor airways allografts had similar amounts of infiltrating leukocytes, destroyed epithelium, and fibroblasts obstructing the airway (Supplemental Figure 1, B and C). Thus, CCR4 expression on host-derived cells participates in promoting allograft rejection.

CCR4^{-/-} SLT have a reduction in the amount of T cells during airway allograft rejection

Based on the HEV and mononuclear phagocytes expressing CCL17 and CCL22 in the allograft draining SLT, we tested the chemokines importance in driving T cell trafficking to the lymph nodes following allograft transplantation. At day 7 post-transplant, a time point with extensive leukocyte infiltration into the allograft (32, 33, 36), we observed a significant reduction in total numbers of CD4⁺ and CD8⁺ T cells, as well as their subpopulations with central memory (CD62L⁺CD44^{high}) and naïve T cell (CD62L⁺CD44^{low/neg}) phenotypes from CCR4^{-/-} recipient lymph nodes as compared to controls (Figure 2, E-G). Interestingly, only the frequency of CD8⁺ T cells and their central memory and naïve T cell phenotypes were reduced, while the frequency of CD4⁺ T cells and their subpopulations of central memory and naïve T cell phenotypes was unchanged in CCR4^{-/-} SLT compared to CCR4^{+/+} controls (Figure 2, H-J, and Supplemental Figure 2, A-C). Some studies have shown that CCR4 expressing regulatory T cells (Treg) are important for tolerance (41, 42), while others have not (43). Thus, we evaluated the expression of Foxp-3; a marker for Tregs (41, 42), in draining lymph node homogenates from the CCR4^{-/-} recipients. There are reductions in Foxp-3 mRNA expression by

qPCR from the CCR4^{-/-}, as compared to CCR4^{+/+} recipient lymph nodes at day 7 (Figure 2, K and L). These results suggest the inhibition of CCR4 with its ligands can decrease Foxp-3 expressing cells in SLT during an allogeneic response. Overall, CCR4 deletion leads to diminished T and Foxp-3 expressing cells within the SLT following allograft transplantation.

CCR4 deficiency on T cells inhibits allograft rejection by preventing T_n homing and activation within the draining SLT

To probe whether CCR4 signaling specifically, on T cells, attenuates allograft rejection, T cells from CCR4^{+/+} or CCR4^{-/-} mice were adoptively transferred pre-transplant (day 0) into CCR4^{+/+} or CCR4^{-/-} recipients. Airway allografts in CCR4^{-/-} recipients receiving CCR4^{-/-} T cells had limited rejection, while airway allografts in CCR4^{-/-} recipients receiving CCR4^{+/+} T cells were rejected similar to CCR4^{+/+} allograft recipients with the adoptive transfer (AT) of CCR4^{+/+} T cells (Figure 3A). Analysis of the airway allograft tissue demonstrate that the CCR4^{-/-} recipients with the AT of CCR4^{-/-} T cells have some intraluminal leukocyte infiltration as well as mucus with cytokeratin and leukocyte debris that is inherent to the heterotopic position of the airway graft (Figure 3B). Importantly, there is minimal epithelial cell injury without any significant fibroblasts obstructing the airway (Figure 3B). In opposition, CCR4^{-/-} recipients with the AT of CCR4^{+/+} T cells are similar to the CCR4^{+/+} recipients receiving CCR4^{+/+} T cells, in which we observe many intraluminal leukocytes and a denuded basement membrane with fibroblasts obstructing the airway (Figure 3B). Thus, CCR4 expression on the T cells is critical for driving allograft rejection, while preventing CCR4–ligand interactions dramatically attenuates graft rejection.

Exploring mechanisms for CCR4 expressing T cells involvement in rejection, CCR4^{+/+} and CCR4^{-/-} T cells from naïve mice were labeled and equal amounts transferred into day 7 CCR4^{+/+}

recipients of airway allografts. Eighteen hours post-transfer, the draining lymph nodes were harvested and processed into single cell suspensions for labeled T cell analysis by flow cytometry. There were dramatic reductions in the frequency of labeled CCR4^{-/-} total T cells as well as CD4 and CD8 T cells in allograft draining nodes, as compared to labeled CCR4^{+/+} T cells and their subpopulations (Figure 3, C-E, and Supplemental Figure 3A). However, if there are certain genetic differences between the CCR4^{-/-} and CCR4^{+/+} T cells, it is possible that the endogenous and transferred CCR4^{+/+} T cells might reject co-transferred CCR4^{-/-} T cells and this would result in a lower recovery of the CCR4^{-/-} T cells within the draining nodes. Thus, we performed the same co-transfer experiments using day 7 CCR4^{-/-} allograft recipients. Again, there were reductions in the frequency of labeled CCR4^{-/-} total T cells, CD4 and CD8 T cells in the CCR4^{-/-} allograft recipient draining nodes, as compared to labeled CCR4^{+/+} T cells and their subpopulations (Figure 3, C-E). However, not to the same magnitude found in the day 7 CCR4^{+/+} recipients, likely due to less rejection found with the CCR4^{-/-} recipients. Furthermore, we found CD62L was downregulated on the majority of labeled CCR4^{+/+} CD4⁺ and CD8⁺ Tn cells in the SLT from the CCR4^{+/+} allograft recipients at 18 hours, while CD62L expression remained high on almost all of the labeled CCR4^{-/-} Tn cell CD4⁺ and CD8⁺ subpopulations (Figure 3F, and Supplemental Figure 3B). There is a possibility that the downregulation of CD62L by CCR4^{+/+} T cells is due to their activation by the CCR4^{-/-} co-transferred T cells if they have certain genetic differences from the CCR4^{+/+} T cells rather than being activated from alloantigens. Hence, we performed the same co-transfer experiment, but into day 7 isografts and found there was no differences in CD62L expression, which remained high on most of the CCR4^{+/+} and CCR4^{-/-} labeled Tn cell subpopulations (Figure 3F), confirming that CCR4^{-/-} as compared to CCR4^{+/+} T cells are having trouble being activated from alloantigens within the draining lymph node. Collectively, these experiments indicate that the CCR4^{-/-} CD4⁺ and CD8⁺ Tn cells during rejection have decreased

ability to home to draining lymph nodes and those CCR4^{-/-} T cells that do make it to the lymph nodes are not being efficiently activated against alloantigens from the airway allograft.

CCR4^{-/-} recipients have a reduction in alloresponsive CD4⁺ and CD8⁺ T cells

The reduction in SLT homing and intranodal activation of CD4⁺ and CD8⁺ Tn cells following allograft transplantation, suggests that CCR4^{-/-} T cells would also exhibit decreased effector function. To test this assumption cells were isolated from the draining SLT 7 days after allograft transplantation from CCR4^{-/-} and CCR4^{+/+} recipients and stimulated with irradiated BALB/c splenocytes. In response to allo-stimulation, CCR4^{+/+} CD4⁺ and CD8⁺ T cells readily produced high amounts of IFN- γ (Figure 3G, and Supplemental Figure 4A). Strikingly, CD4⁺ and CD8⁺ T cells from CCR4^{-/-} mice produced almost no IFN- γ in response to allo-stimulation despite the graft having been transplanted 7 days earlier (Figure 3G, and Supplemental Figure 4A). Importantly, both CCR4^{-/-} and CCR4^{+/+} SLT CD4⁺ and CD8⁺ T cells from naïve mice exhibited similar responses to the superantigen Staphylococcal Enterotoxin B with regard to IFN- γ production, demonstrating that CCR4^{-/-} T cells do not have an intrinsic activation defect (Supplemental Figure 4, B and C).

To further test the induction of the allograft response, we used an in vivo delayed type hypersensitivity (DTH) response to alloantigens as a physiologic readout of alloprimed cells (44, 45). Irradiated BALB/c splenocytes were administered intradermally to the pinnae of: (1) CCR4^{-/-} allograft recipients at day 7 after transplant; (2) CCR4^{+/+} allograft recipients at day 7 after transplant; (3) naïve CCR4^{-/-}; or (4) naïve CCR4^{+/+} mice. CCR4^{-/-} allograft recipients displayed a markedly reduced DTH response compared to CCR4^{+/+} allograft recipients (Figure 3H). Furthermore, the response was reduced to the level of that seen in the naïve CCR4^{-/-} and naïve CCR4^{+/+} mice (Figure 3H), indicating minimal functionally active alloresponsive T cells in the absence of CCR4 expression.

We further explored the down-stream effects of CCR4-ligand inhibition on T cell function within the airway allograft. Interestingly, the frequency of allograft infiltrating CD4⁺ T cells in CCR4^{-/-} mice was significantly increased, whereas the frequency of CCR4^{-/-} CD8⁺ T cells was markedly decreased compared to CCR4^{+/+} mice 7 days after allograft transplantation (Figure 4A). Upon further analysis there was no difference in CD44^{high} CD4⁺ CD62L⁻ T cells and a reduction in the frequency of CD44^{high} CD8⁺ CD62L⁻ T cells in the allografts from the CCR4^{-/-} recipients as compared to the CCR4^{+/+} recipients (Figure 4B). Furthermore, the protein levels of IL-2, TNF- α and IFN- γ , and the mRNA levels of the T cell killing effectors FasL and perforin were also decreased in the airway allografts of CCR4^{-/-} mice as compared to the CCR4^{+/+} recipients (Figure 4, C-G). In contrast, there was no significant difference in the mRNA expression of Foxp-3 in airway allografts from CCR4^{-/-} and CCR4^{+/+} recipients (Figure 4H). Thus, in the absence of CCR4 expression, there is a dramatically diminished ability for T cells to mount functional responses against airway allografts, despite being present in the transplanted tissue.

Allograft rejection is dependent on help from CCR4^{+/+} CD4⁺ T cells, not NKT or CCR4^{+/+} CD8⁺ T cells

A recent study has demonstrated that natural killer T (NKT) cell help, via a CCR4 dependent mechanism, is important during ova sensitization (26) and this may apply to allograft rejection. However, we observed no difference in airway rejection scores at days 7 and 21 between Cd1d1^{-/-} recipients that lack NKT cells as compared to Cd1d1^{+/+} recipients (Supplemental Figure 5, A and B). To determine if other subsets of T cells functioned in a CCR4 dependent mechanism to induce allograft rejection, we adoptively transferred CCR4^{+/+} CD4⁺ T cells, CD8⁺ T cells, or total T cells into CCR4^{-/-} recipients just prior to airway transplantation. At day 21 post-transplant, the CCR4^{-/-} recipients

receiving either CCR4^{+/+} or CCR4^{-/-} CD8⁺ T cells exhibited a similarly low rejection score (Figure 5A, and Supplemental Figure 5C). Interestingly, CCR4^{-/-} recipients receiving CCR4^{+/+} CD4⁺ T cells re-established a significant portion of alloreactivity with rejection scores markedly greater than transferred CCR4^{-/-} CD4⁺ T cells, but not as high as the scores found with the transfer of total T cells to the CCR4^{-/-} recipients (Figure 5, B and C). Furthermore, when CCR4^{+/+} CD4⁺ T cells were transferred to CCR4^{-/-} recipients with either control Ab or the depleting anti-CD8 Ab delivered at days -1, 7 and 14, there was a reduction in rejection scores with the anti-CD8 Ab treated group at day 21 (Figure 5, D and E). Collectively, these results imply that maximal allograft rejection is present when CCR4 expression is on both CD4⁺ and CD8⁺ T cells and suggest that CCR4 expressing CD4⁺ T cells can directly cause a degree of allograft injury as well as provide help to CD8⁺ T cells during allograft rejection.

CCR4 deletion in combination with CTLA4-Ig leads to long-term airway and lung allograft accommodation

The combination of anti-CD154 (CD40L) with CTLA4-Ig to inhibit T cell priming is considered the preeminent combination used to induce long-term allograft accommodation (46). Therefore, we hypothesized that CCR4-ligand inhibition by decreasing T cell priming and activation may have a similar therapeutic potential as anti-CD154 to enhance CTLA4-Ig immunotherapy. Accordingly, we evaluated the effects of CCR4^{-/-} allograft recipients receiving CTLA4-Ig therapy on allograft survival. CTLA4-Ig (0.2 mg) i.p. was given on day 0 prior to transplant and at days 2, 4 and 6 post-transplant to CCR4^{-/-} or CCR4^{+/+} recipients of BALB/c airways. Strikingly, the allograft airways from the CCR4^{-/-} recipients are virtually normal at days 42 and 126; whereas the allograft airways from the CCR4^{+/+} recipients were completely rejected and fibro-obliterated by day 42 (Figure 6, A and B, Supplemental Figure 6A). Thus, CCR4 deficiency in

combination with a short peri-operative course of CTLA4-Ig enabled an unprecedented long-term allograft survival in a situation that normally leads to rejection in a month.

We next performed proof of concept studies using the fully mismatched, vascularized left single lung transplant model via the same stringent strain combination (BALB/c lung to C57BL/6 recipients) as the airway allograft model to corroborate our results. Lung allografts in CCR4^{+/+} recipient mice treated with CTLA4-Ig (0.1 mg) i.p. just prior to transplant developed severe grade A rejection ($AR \geq 3$) with or without vasculitis, severe grade B rejection ($B \geq 3$) with high-grade infiltrates and epithelial cell injury, and severe pleural and septal inflammation with and without fibrosis by day 126 post-transplant (Figure 6C). In contrast, CCR4^{-/-} recipients treated with the same single dose of pre-transplant CTLA4-Ig (0.1 mg) had virtually normal lung allografts without any significant pathology at day 126 (Figure 6D). Quantitatively, CCR4^{+/+} versus CCR4^{-/-} recipients with a single pre-transplant low dose of CTLA4-Ig, allograft scores are (AR: 100% vs 0%; $p=0.008$), (LB: 100% vs 0%; $p=0.008$), (pleural involvement: 60% vs 0%; $p=0.17$), (septal involvement: 80% vs 0%; $p=0.04$); respectively. Thus, CCR4 deficiency in combination with an initial CTLA4-Ig treatment at the time of transplantation enabled long-term lung allograft accommodation.

Discussion

Median survival for solid organ transplants such as liver, kidney and hearts is greater than 10 years; regrettably this falls to less than 5 years for lung transplant recipients (1-6). The “Achilles heel” for lung transplant is chronic lung allograft dysfunction, which is predominately do to rejection (7, 9, 11, 47, 48). Unfortunately, our current immunosuppressive strategies have been ineffective for long-term lung allograft accommodation (7, 9, 11, 47, 48), which mandates the need for new insights into lung alloreactivity. Using stringent animal models of airway and lung allograft rejection, we demonstrate

that the CCR4-ligand biological axis is central to the allopriming that leads to graft rejection and that CCR4 deficiency dramatically abolishes rejection by restricting nodal homing and subsequent intranodal activation of CD4⁺ and CD8⁺ Tn cells. Both CCR4 expressing CD4 and CD8 T cells are critical for rejection, but the CD4⁺ T cells were pivotal for helping generate alloresponsive cytotoxic T cells that trigger rapid rejection. Excitingly, CCR4 deficiency combined with a low dose CTLA4-Ig immunotherapy at the time of airway transplantation enabled an unprecedented long-term allograft survival to over 125 days, over 3 times longer than CTLA4-Ig alone. This was corroborated using the orthotopic lung transplant model. Thus, this study demonstrates for the first time, a molecular mechanism involving one specific chemokine axis required for homing and intranodal activation of allo-specific CD4⁺ and CD8⁺ Tn cells that mediate graft rejection. Importantly, inhibition of this chemokine axis with CTLA4-Ig allows for long-term allograft survival.

SLT are strategically positioned at the interface between the blood and the lymphatic system and provides an environment that allows for the exchange of antigenic information between cells of the innate and adaptive immune system (49, 50). However, the crowding of immune cells in the SLT suggests a role for chemokine guidance in optimizing adaptive immunity (49-51). Many studies suggest chemokine redundancy limits the usefulness of targeting a single chemokine axis to significantly impair T cell priming (16-22). However, we were struck by the marked elevations of the CCR4 ligands from the allograft SLT. This led to our hypothesis that these chemokines could be key regulators of allopriming.

Importantly, we found CCR4^{-/-} allograft recipients had an unprecedented prolonged reduction in rejection when compared to other chemokine axes (32, 33, 36). This suggests that inhibition of allopriming has the potential for a superior transplant outcome as contrasted to trying to limit the consequences of allo-specific T cells that were already generated (32, 33, 36). Mechanistically, we

ruled out any significant effect of CCR4 expression on donor cells in direct rejection, which focused our attention on recipient CCR4 expressing T cells during allopriming.

Post-transplant, draining nodes express CCL17 localized to HEV and CCL22 from subcapsular sinus mononuclear phagocytes, which is consistent with our adoptive transfer studies demonstrating that CCR4 expression from Tn ($CD4^+$ and $CD8^+$) was fundamental for proper homing during allopriming. Furthermore, the expression of CCL22 from paracortical mononuclear phagocyte in close proximity to HEV, in combination with our data indicating that the few CCR4^{-/-} $CD4^+$ and $CD8^+$ Tn cells that make it the SLT have trouble shedding CD62L, is consistent with a reduction in CCR4^{-/-} Tn cell interactions with APC surrounding HEV (17). Collectively, these studies corroborate that the CCR4-ligand biological axis is unique in its importance for both $CD4^+$ and $CD8^+$ Tn cells to home to SLT, and for intranodal activation needed for the optimal generation of alloresponsive T cells.

Our findings are consistent with the importance of CCR4 expression on other lymphocytes such as NKT cells, as was shown during ova sensitization (26). More specifically, CCR4 ligands were expressed by APC within SLT, which optimized their interactions with NKT cells; that in turn, licensed the APC to express CCL3 and CCL4 calling in CCR5⁺ $CD8^+$ T cells, ultimately generating ova specific cytotoxic T lymphocytes (26). Thus, we explored the role of NKT cells during allograft rejection through the use of genetically altered mice that lack NKT cells (i.e., Cd1d1^{-/-} mice) as allograft recipients. However, we found no difference in early or late allograft rejection, essentially negating any substantial role of CCR4 expressing NKT cells during rejection.

We noted that the CCR4^{-/-} allograft recipients had a greater reduction in the frequency of $CD8^+$ T cells as compared to $CD4^+$ T cells in both the allografts and SLT, which led us to evaluate if CCR4 expression on $CD8^+$ T cells could lead to $CD8^+$ T cell help in generating more allo-injurious T cells. However, adoptive transfer studies did not establish any CCR4^{+/+} $CD8^+$ T cell help with regard to

rejection. Conversely, we did find that CCR4 expression on CD4⁺ T cells was important for CD4⁺ T cell help in generating an alloreactive response causing rejection. Taken together, our adoptive transfer studies demonstrate a hierarchy of CCR4^{+/+} lymphocytes with respect to re-establishing rejection in the CCR4^{-/-} recipients (CCR4^{+/+} CD90.2 > CCR4^{+/+} CD4⁺ T cells > CCR4^{+/+} CD8⁺ T cells). Importantly, perturbing allopriming via CCR4-ligand interruption had physiologic consequences such as a marked reduction in the clonal expansion of both CD4⁺ and CD8⁺ alloresponsive T cells, decreased in vivo DTH response to alloantigens, and diminished cytotoxic T cell down-stream pathways at the site of the allograft. Taken together with other studies (31-34, 52), our study suggests CCR4-ligand interaction is a linchpin in the alloresponse, and inhibition of this single chemokine axis can limit allograft rejection.

Rodent models of allograft rejection have demonstrated that the most impressive therapy that allows for long-term allograft acceptance was the combined costimulatory blockade involving anti-CD154 and CTLA4-Ig (46). Unfortunately, human studies involving anti-CD154 led to high rates of vessel thrombosis (53, 54) quickly dampening the hopes for a strategy to achieve long-term accommodation. However, our data suggests that the inhibition of CCR4-ligand interactions is an alternate method to limit costimulation between CD4⁺ Tn cells and APC. Thus, we tested the combination of a short course of CTLA4-Ig with either the CCR4^{-/-} or CCR4^{+/+} recipients and found that CCR4^{-/-} recipients have virtually normal airway allografts at day 126, while CCR4^{+/+} recipients were completely rejected by day 42. Importantly, this was reproducible in the vascularized orthotopic single lung transplant model as CTLA4-Ig given to CCR4^{-/-} recipients rendered a virtually normal lung allograft at day 126.

Interestingly, two studies have evaluated CCR4 expressing Tregs in cardiac allograft models that develop tolerance via the combination of inhibiting CD40-CD154 interactions (eg, anti-CD154 Ab)

with a donor splenocyte transfusion (DST) (41, 42). In the first study, the Treg expression marker Foxp-3 was found to be elevated in the allografts from recipients with tolerance, as compared to allografts with long-term accommodation (eg, CD28^{-/-} recipient plus anti-ICOS mAb therapy) or allografts undergoing acute rejection (eg, no immunosuppression) (41). Importantly, when the tolerizing therapy (anti-CD154 with DST) was applied to CCR4^{-/-} and CCR4^{+/+} recipients the allografts Foxp-3 expression was significantly lower from the CCR4^{-/-} recipients (41), which translated into a reduction in allograft survival (41). The second study involved a similar cardiac tolerance model and found CCR7 expressing plasmacytoid dendritic cells move from the allograft to the lymph node, then secrete CCL17 and TGF- β . CCL17 then recruits conventional T cells expressing CCR4, while the TGF- β induces these T cells into Treg allowing tolerance to occur (55). Importantly, anti-CD154 and the DST could not provoke tolerance when delivered to the CCR4^{-/-} allograft recipients (55). Another study involving an islet cell transplant model that is exquisitely sensitive to Treg therapy for tolerance (56) found CCR4 expression to be important for Treg movement from the blood to the allograft, where they become activated and then expressed CCR7, IL-10 and TGF- β . The cytokines inhibited dendritic cell migration from the allograft to the draining lymph node, while CCR7 expression lead to Treg homing to the draining node, which reduced alloresponsive T cells (57). In a fully mismatched model of cardiac transplantation the use of CCR4^{-/-} recipients trended toward prolonged allograft survival (p=0.05) (58), while the addition of the immunosuppressive drug Gallium nitrate (GN) lead to a reduction in allograft infiltrating lymphocytes and significantly prolonged allograft survival (58). Collectively, these studies in combination with our results demonstrate that CCR4 expression from CD4⁺ T cells (conventional and Treg) may have disparate properties depending on the allograft environment. More specifically, CCR4 expression is important for Treg to induce tolerance at the nodal and allograft levels. However, in an accommodating environment CCR4

expressing CD4⁺ T cells are important for homing and intranodal trafficking that generate alloresponse T cells as well as Foxp-3 expression within SLT. Thus, it is conceivable that CCR4 inhibition in human lung transplant recipients receiving standard triple immunosuppressive therapy could reduce alloresponsive T cells, while reducing Foxp-3 expression within SLT. This should reduce and delay rejection thereby promoting long-term accommodation. However, this may occur at the expense of giving the lung allograft any chance of cultivating donor specific tolerance.

In conclusion, we have found that interrupting allopriming by manipulating CCR4-ligand interactions causes both CD4⁺ and CD8⁺ Tn cells to have difficulties homing to SLT, as well as their activation within the node. This leads to a dramatic reduction in the clonal expansion of alloresponsive T cells, DTH response, and cytotoxic mediators, which markedly attenuates allograft rejection. Moreover, the combination of CCR4-ligand inhibition with CTLA4-Ig blockade leads to long-term accommodation that outperforms the best known combination of costimulatory blockade (anti-CD154 and CTLA4-Ig) (46). Overall, this study suggests that altering events prior to allorecognition, or the so called “Signal 0”, via the CCR4-ligand biological axis may be a therapeutic option to prolong allograft survival and warrants further investigation in human organ transplantation.

Methods

Animals. Wild-type female BALB/c (H-2K^d), C57BL/6 (H-2K^b), and B6(C)-Cd1d1^{tm1.2Aben/J} (NKT^{-/-}) mice, 8-10-week-old, were purchased from The Jackson Laboratories (Bar Harbor, ME, USA). CCR4^{-/-} mice on a C57BL/6 background were kindly provided by Dr. Cory Hogaboam (Cedars-Sinai, Los Angeles, CA).

Murine Rejection Models. Heterotopic subcutaneous tracheal/airway transplantation model of alloreactivity involves the most stringent MHC class I-and II-disparate combination mismatch found in mice: BALB/c (H-2^d) tracheas transplanted subcutaneously into the upper backs of C57BL/6 (H-2^b) mice (allografts), and C57BL/6 tracheas transplanted subcutaneously into the backs of C57BL/6 mice (syngeneic control) (32, 33, 36). Each mouse was subcutaneously transplanted with two tracheas. Small molecule CCR4 antagonist C 021 dihydrochloride (Cat # 3581, Tocris Bio-Techne, Minneapolis, MN, USA) was resuspended in sterile DMSO to 100 mg/ml and diluted further in 1x PBS to be administered as intraperitoneal (i.p.) injections at 50 mg/kg daily starting at day -1 prior to tracheal transplantation until day 14 when allografts were harvested for rejection analysis. For long-term experiments, CTLA4-Ig treatment (Bristol-Myers Squibb Company, Princeton, New Jersey, USA) was given as 0.2 mg i.p. injection on day 0 prior to tracheal transplantation and at days 2, 4 and 6 thereafter.

The orthotopic left single lung transplant model involved BALB/c left lungs transplanted into CCR4^{+/+} or CCR4^{-/-} recipients in combinations with a single pre-operative dose of 0.1 mg CTLA4-Ig using a modification of the rodent left lung transplant procedure previously described (36, 52). Briefly, donor BALB/c mice were anesthetized, intubated, ventilated and the left lung harvested and Teflon cuffs secured on the pulmonary artery, vein and bronchus then covered with

soaked gauze pads on ice. The recipient mice are anesthetized, intubated, and ventilated. A 2-cm incision is made between 3-4 ribs on the left and a 1/4-binder clip placed to expose the posterior hilum. Appropriate dissection of the hilum components included ligation and clamping after heparin delivery. A donor lung is inserted using the cuff technique via 10.0 ethilon suture. Incisions closure involved v6-0 surgical suture. During the procedure 1 cc of saline is administered subcutaneously and post-operatively the animals are placed in cages on warm water mattresses until recovered from anesthesia. Buprenorphine 0.1 mg/kg i.p. is given every 12 hours while monitoring for pain. Sutures are removed on post-operative day 7.

Histopathological Evaluation of Airway and Lung Transplants. Airway and lung graft tissues were fixed overnight in 4% paraformaldehyde, processed and paraffin-embedded by the Translational Pathology Core Laboratory at UCLA, and sectioned and stained with hematoxylin and eosin (H&E) or Elastin Trichrome. Three independent blinded reviewers calculated the degree of airway injury using the histological scoring system as described previously (32, 33, 36). All qualitative histological changes were evaluated and the total murine rejection score was calculated based on four pathological criteria: (a) airway lining epithelial loss, (b) deposition of extracellular matrix (ECM), (c) leukocyte infiltration, and (d) luminal fibro-obliteration due to granulation tissue formation and/or fibrosis. Each process was scored on a scale of 0–4 (0 = normal, 1 = mild, 2 = moderate, 3 = severe and 4 = very severe) and added together for a total rejection score. Lung allograft rejection scores included acute rejection, lymphocytic bronchiolitis, pleural and septal rejection based on established criteria (59, 60). Images were taken by Zeiss Axioskop 2 plus microscope and analyzed with AxioVision 4.2 imaging software (Carl Zeiss Microscopy, LLC, Thornwood, NY, USA). Images were taken as 5x to show whole pathology of tracheas and as 20x

to amplify presence or absence of either epithelial cells and/or fibro-obliteration of the airway allograft lumen as well as different aspects of lung rejection and fibrosis.

Immunohistochemistry. Staining of paraffin-embedded lymph node samples was performed using the VECTASTAIN ABC Standard kits (Vector Laboratories, Inc., Burlingame, CA, USA) as previously described (61). After deparaffinization and antigen retrieval in sodium citrate buffer (pH 6.0), endogenous peroxidase was quenched with 3% hydrogen peroxide. Tissues were incubated in appropriate blocking serum and endogenous biotin was blocked with an avidin/biotin blocking kit (Vector Laboratories, Inc., Burlingame, CA, USA). Slides were incubated overnight with primary antibodies at 4°C. The primary antibodies for rat polyclonal anti-mouse CCL17 (MAB529) were purchased from R&D Systems Inc. (Minneapolis, MN, USA) and rabbit monoclonal anti-mouse CCL22 (ab124768) were purchased from Abcam (Cambridge, MA, USA). Specific labeling was detected with a biotinylated specific secondary antibody and application of horseradish peroxidase-conjugated avidin-biotin followed by visualization with DAB solution (Vector Laboratories, Inc., Burlingame, CA, USA).

Total RNA isolation and real-time quantitative PCR. Total cellular RNA from transplanted airways (previously frozen in liquid nitrogen) was isolated using Trizol (Thermo Fisher Scientific, Grand Island, NY, USA) and chloroform treatment, precipitated with isopropanol, washed twice with 75% ethanol and resuspended in DEPC-treated water. Total RNA concentration was determined using Nanodrop 2000 UV-Vis spectrophotometer (Thermo Fisher Scientific, Grand Island, NY, USA) and 2 µg of total RNA was DNase-treated to remove genomic DNA contamination and reversed transcribed into cDNA using Taqman reverse transcription reagents (Thermo Fisher Scientific, Grand Island, NY, USA). Specific targets were amplified on StepOnePlus qPCR

machine (Thermo Fisher Scientific, Grand Island, NY, USA) using Taqman gene expression assays: Perforin 1 (Mm00812512_m1), Fas-ligand (Mm00438864_m1), Foxp-3 (Mm00475156_m1) and Eukaryotic 18S (4319413E) as an endogenous control. The RNA expression levels were compared to wild-type allografts using $2^{\Delta\Delta Ct}$ method (62) and visualized as fold difference to allografts.

Protein Analysis by Luminex. Draining lymph nodes and heterotopically transplanted airways from recipient animals were surgically removed on different days (7, 14 and 21 days) and snap frozen in liquid nitrogen. Frozen tissues were homogenized in 1x PBS supplemented with complete protease inhibitor cocktail (Roche, Indianapolis, IN, USA), sonicated on ice for 10 seconds, centrifuged at 13,000 rpm to remove any cellular debris and analyzed by Luminex labeling kits (R&D Systems Inc. Minneapolis, MN, USA) using manufacturer's instructions.

Flow Cytometry Analysis of draining lymph nodes and airway allografts. Single-cell suspension was prepared from harvested axillary/brachial lymph nodes or airways using a method described previously (32, 33, 36). Briefly, tissues were put through a steel mesh by using a plunger and cells were collected in RPMI-1640 media (Mediatech, Manassas, VA, USA) supplemented with L-glutamine, penicillin/streptomycin and HEPES buffer. Red blood cells were lysed using ACK (Ammonium-Chloride-Potassium) lysing buffer and washed twice in 1x PBS + 0.1% FBS. Live cells counted with hemocytometer using trypan blue (Sigma-Aldrich, St. Louis, MO, USA) and 1×10^6 cells were stained with different cell surface conjugated anti-mouse antibodies: hamster CD3a-PerCP, CD3a-FITC, rat CD4-FITC, CD4-APC, CD8-FITC, CD8a-APC, CD44-APC, and CD62L-PE (BD Biosciences, Franklin Lakes, NJ, USA). The cell suspensions were acquired using

FACSCalibur (BD Biosciences, San Jose, CA, USA), analyzed with CellQuest software (BD Biosciences, San Jose, CA, USA) and data was expressed and compared as frequencies of selected subpopulations. The specific gating strategies for each experiment are explained in figure captions where appropriate.

Flow cytometry IFN- γ cytokine secretion assay (FCIS). A mixture of draining lymph node (axillary/brachial) cells from CCR4^{-/-} and CCR4^{+/+} airway allograft recipients at day 7 were collected for ex vivo stimulation. Single cell suspension was prepared as described previously and 1×10^6 recipient cells from CCR4^{-/-} and CCR4^{+/+} allograft recipients, naïve non-transplanted CCR4^{-/-} and CCR4^{+/+} mice were stimulated in the presence of either RPMI 1640 supplemented with 5% FBS alone or with 2×10^6 irradiated and digested BALB/c splenocytes. After 16 hours of incubation at 37°C and 5% CO₂, cells were washed and analyzed using the flow cytometry IFN- γ cytokine secretion assay (Miltenyi Biotec Inc. San Diego, CA, USA) via flow cytometry analysis on a minimum of 250,000 total events. The cells were stained for (7-AAD (to exclude dead cells in PerCP channel), B220-PerCP (to exclude B cells), CD3-FITC, IFN- γ -PE and either CD4-APC or CD8-APC) to measure % cell frequency of alloresponsive T cells. The coefficient of variation with FCIS is 5-15% with a lower limit of detection of 0.01% or 1/10,000 IFN- γ secreting cells (63).

In vivo delayed-type hypersensitivity (DTH) response. Recipient animals (CCR4^{+/+} and CCR4^{-/-}) post-airway transplant at day 7 were challenged with BALB/c alloantigens in a DTH response using the pinnae swelling assay (64). Briefly, at 7 days' post-transplant a 10 μ l volume of irradiated single-cell suspension of digested BALB/c splenocytes (7.5×10^6 total cells in saline) was injected

in the right ear pinna, by using a 30-gauge needle and a Hamilton syringe (Hamilton, Reno, Nev.). The left control ear pinna received 10 μ l of sterile saline solution. Ear swelling was measured 48 hours later with a Mitutoyo 7326 Micrometer (Schlessinger Tools, New York, N.Y.), and the results were expressed as the mean swelling of challenge ear minus the mean swelling of control ear (units, mm). All challenges and measurements were performed under light anesthesia (isoflurane).

Adoptive transfer experiments. Total (CD90.2⁺), CD4⁺ or CD8⁺ T cells were purified from spleens of naïve CCR4^{+/+} or CCR4^{-/-} mice by positive selection using CD90.2, CD4(L3T4) or CD8(Ly-2) T cell Microbead Isolation Kits, respectively (Miltenyi Biotec Inc. San Diego, CA, USA) following manufacturing instructions. Briefly, animal spleens were surgically extracted and pushed through metal mesh to remove cells and washed twice in MACS rinsing buffer supplemented with 2% BSA. Total cells were counted using Crystal Violet and stained with MicroBeads and purified using positive selection by magnetic LS columns (Miltenyi Biotec Inc. San Diego, CA, USA), washed and resuspended in sterile saline. After selection, 1×10^7 CD90.2, 5×10^6 of CD4⁺ or 5×10^6 of CD8⁺ live T cells (as determined by trypan blue staining) were injected i.v. into each mouse prior to subcutaneous transplantation with BALB/c tracheas. Allograft rejection was analyzed at day 21 by histopathological rejection scoring analysis as previously described. Additionally, we performed in vivo CD8⁺ T cell depletion experiments. CCR4^{-/-} mice were given an i.p. injection of either 0.25 mg of anti-CD8 antibody (clone 53-6.72, BioXCell, West Labanon, NH) or control isotype antibody (clone 2A3, BioXCell, West Labanon, NH) at day -1 of heterotopic BALB/c transplant and repeated at days 7 and 14 post-transplant with the addition of

a transfer of 5×10^6 CD4⁺ T cells injected immediately prior to heterotopic transplant procedure. Allografts were isolated at day 21 and evaluated for rejection.

T-cell trafficking. Splenic total T cells were purified from naïve CCR4^{+/+} or CCR4^{-/-} animals and labeled with 4.0 μ M of CFSE (Thermo Fisher Scientific, Grand Island, NY, USA) or 0.25 μ M of CFSE, respectively, by manufacturer's instructions. Stained single cell suspensions were washed three times in cold 1x PBS/1%BSA to remove residuals of CFSE, resuspended in sterile saline and mixed as a 1:1 ratio of live cells as determined by trypan blue counts. 10×10^6 live total T-cells per 150 μ l of sterile saline were injected into (1) day 7 CCR4^{+/+} or CCR4^{-/-} recipients transplanted with BALB/c airways and (2) day 7 CCR4^{+/+} recipients transplanted with C57BL/6 airways (isogeneic). Axillary/brachial lymph nodes were removed after 18 hours and analyzed by flow cytometry for different T cell subpopulations.

Statistics. Data were analyzed using GraphPad Prism 7.00 statistical software (GraphPad Software, La Jolla, CA, USA, www.graphpad.com). Group comparisons were evaluated by the unpaired two-tailed t-test or Mann-Whitney where appropriate for statistical significance and reported as mean \pm standard error of the mean (SEM). Multiple comparisons were performed with the Kruskal-Wallis and post-hoc Dunn. $p < 0.05$ is considered statistically significant.

Study approval. All animals were housed in the animal husbandry at UCLA facilities and experiments were conducted under a protocol approved by Animal Care Committee in accordance to federal, state, and local regulations.

Author contributions

VP, MK, JB designed experiments, VP, YYX, RK, MK and JB performed experiments. VP, SW, AG, SS, MF, CH, DS, JL, MK, DB and JB analyzed the data. VP and JB wrote the manuscript.

Acknowledgements

We would like to thank Dr. Elaine Reed and Dr. Yael Korin for assistance with learning the FCIS assay. We also thank Dr. Shirin Birjandi, Dr. Angela Wong and Wing Yi Lung for their valuable suggestions and assistance regarding experimental procedures. This study was supported in part by NIH funding that includes R01 HL112990 and P01HL108793-06 to J.A.B.

References:

1. Chambers DC, Yusen RD, Cherikh WS, Goldfarb SB, Kucheryavaya AY, Khusch K, et al. The Registry of the International Society for Heart and Lung Transplantation: Thirty-fourth Adult Lung And Heart-Lung Transplantation Report-2017; Focus Theme: Allograft ischemic time. *J Heart Lung Transplant.* 2017;36(10):1047-59.
2. Hart A, Smith JM, Skeans MA, Gustafson SK, Wilk AR, Robinson A, et al. OPTN/SRTR 2016 Annual Data Report: Kidney. *Am J Transplant.* 2018;18 Suppl 1:18-113.
3. Kim WR, Lake JR, Smith JM, Schladt DP, Skeans MA, Harper AM, et al. OPTN/SRTR 2016 Annual Data Report: Liver. *Am J Transplant.* 2018;18 Suppl 1:172-253.
4. Lodhi SA, Lamb KE, and Meier-Kriesche HU. Solid organ allograft survival improvement in the United States: the long-term does not mirror the dramatic short-term success. *Am J Transplant.* 2011;11(6):1226-35.
5. Lund LH, Edwards LB, Dipchand AI, Goldfarb S, Kucheryavaya AY, Levvey BJ, et al. The Registry of the International Society for Heart and Lung Transplantation: Thirty-third Adult Heart Transplantation Report-2016; Focus Theme: Primary Diagnostic Indications for Transplant. *J Heart Lung Transplant.* 2016;35(10):1158-69.
6. Rana A, Gruessner A, Agopian VG, Khalpey Z, Riaz IB, Kaplan B, et al. Survival benefit of solid-organ transplant in the United States. *JAMA Surg.* 2015;150(3):252-9.
7. Belperio JA, Weigt SS, Fishbein MC, and Lynch JP, 3rd. Chronic lung allograft rejection: mechanisms and therapy. *Proc Am Thorac Soc.* 2009;6(1):108-21.
8. Shino MY, Weigt SS, Li N, Derhovanessian A, Sayah DM, Huynh RH, et al. Impact of Allograft Injury Time of Onset on the Development of Chronic Lung Allograft Dysfunction After Lung Transplantation. *Am J Transplant.* 2016.
9. Shino MY, Weigt SS, Li N, Palchevskiy V, Derhovanessian A, Saggarr R, et al. CXCR3 ligands are associated with the continuum of diffuse alveolar damage to chronic lung allograft dysfunction. *Am J Respir Crit Care Med.* 2013;188(9):1117-25.
10. Weigt SS, DerHovanessian A, Wallace WD, Lynch JP, 3rd, and Belperio JA. Bronchiolitis obliterans syndrome: the Achilles' heel of lung transplantation. *Semin Respir Crit Care Med.* 2013;34(3):336-51.
11. Weigt SS, Wallace WD, Derhovanessian A, Saggarr R, Saggarr R, Lynch JP, et al. Chronic allograft rejection: epidemiology, diagnosis, pathogenesis, and treatment. *Semin Respir Crit Care Med.* 2010;31(2):189-207.
12. Weigt SS, Wang X, Palchevskiy V, Gregson AL, Patel N, DerHovanessian A, et al. Gene Expression Profiling of Bronchoalveolar Lavage Cells Preceding a Clinical Diagnosis of Chronic Lung Allograft Dysfunction. *PLoS One.* 2017;12(1):e0169894.
13. Freese DK, Snover DC, Sharp HL, Gross CR, Savick SK, and Payne WD. Chronic rejection after liver transplantation: a study of clinical, histopathological and immunological features. *Hepatology.* 1991;13(5):882-91.
14. Matas AJ. Risk factors for chronic rejection--a clinical perspective. *Transpl Immunol.* 1998;6(1):1-11.
15. Tullius SG, and Tilney NL. Both alloantigen-dependent and -independent factors influence chronic allograft rejection. *Transplantation.* 1995;59(3):313-8.
16. Bajenoff M, Egen JG, Koo LY, Laugier JP, Brau F, Glaichenhaus N, et al. Stromal cell networks regulate lymphocyte entry, migration, and territoriality in lymph nodes. *Immunity.* 2006;25(6):989-1001.
17. Bousso P, and Robey E. Dynamics of CD8+ T cell priming by dendritic cells in intact lymph nodes. *Nat Immunol.* 2003;4(6):579-85.
18. Lindquist RL, Shakhar G, Dudziak D, Wardemann H, Eisenreich T, Dustin ML, et al. Visualizing dendritic cell networks in vivo. *Nat Immunol.* 2004;5(12):1243-50.

19. Mempel TR, Henrickson SE, and Von Andrian UH. T-cell priming by dendritic cells in lymph nodes occurs in three distinct phases. *Nature*. 2004;427(6970):154-9.
20. Miller MJ, Hejazi AS, Wei SH, Cahalan MD, and Parker I. T cell repertoire scanning is promoted by dynamic dendritic cell behavior and random T cell motility in the lymph node. *Proc Natl Acad Sci U S A*. 2004;101(4):998-1003.
21. Miller MJ, Wei SH, Cahalan MD, and Parker I. Autonomous T cell trafficking examined in vivo with intravital two-photon microscopy. *Proc Natl Acad Sci U S A*. 2003;100(5):2604-9.
22. Miller MJ, Wei SH, Parker I, and Cahalan MD. Two-photon imaging of lymphocyte motility and antigen response in intact lymph node. *Science*. 2002;296(5574):1869-73.
23. Huang JH, Cardenas-Navia LI, Caldwell CC, Plumb TJ, Radu CG, Rocha PN, et al. Requirements for T lymphocyte migration in explanted lymph nodes. *J Immunol*. 2007;178(12):7747-55.
24. Castellino F, Huang AY, Altan-Bonnet G, Stoll S, Scheinecker C, and Germain RN. Chemokines enhance immunity by guiding naive CD8+ T cells to sites of CD4+ T cell-dendritic cell interaction. *Nature*. 2006;440(7086):890-5.
25. Hugues S, Scholer A, Boissonnas A, Nussbaum A, Combadiere C, Amigorena S, et al. Dynamic imaging of chemokine-dependent CD8+ T cell help for CD8+ T cell responses. *Nat Immunol*. 2007;8(9):921-30.
26. Semmling V, Lukacs-Kornek V, Thaiss CA, Quast T, Hochheiser K, Panzer U, et al. Alternative cross-priming through CCL17-CCR4-mediated attraction of CTLs toward NKT cell-licensed DCs. *Nat Immunol*. 2010;11(4):313-20.
27. Priyadarshini B, Greiner DL, and Brehm MA. T-cell activation and transplantation tolerance. *Transplantation reviews*. 2012;26(3):212-22.
28. Song K, Rabin RL, Hill BJ, De Rosa SC, Perfetto SP, Zhang HH, et al. Characterization of subsets of CD4+ memory T cells reveals early branched pathways of T cell differentiation in humans. *Proc Natl Acad Sci U S A*. 2005;102(22):7916-21.
29. Brandes M, Legler DF, Spoerri B, Schaerli P, and Moser B. Activation-dependent modulation of B lymphocyte migration to chemokines. *Int Immunol*. 2000;12(9):1285-92.
30. Ross R, Ross XL, Ghadially H, Lahr T, Schwing J, Knop J, et al. Mouse langerhans cells differentially express an activated T cell-attracting CC chemokine. *J Invest Dermatol*. 1999;113(6):991-8.
31. Belperio JA, Keane MP, Burdick MD, Gomperts B, Xue YY, Hong K, et al. Role of CXCR2/CXCR2 ligands in vascular remodeling during bronchiolitis obliterans syndrome. *J Clin Invest*. 2005;115(5):1150-62.
32. Belperio JA, Keane MP, Burdick MD, Lynch JP, 3rd, Xue YY, Berlin A, et al. Critical role for the chemokine MCP-1/CCR2 in the pathogenesis of bronchiolitis obliterans syndrome. *J Clin Invest*. 2001;108(4):547-56.
33. Belperio JA, Keane MP, Burdick MD, Lynch JP, 3rd, Xue YY, Li K, et al. Critical role for CXCR3 chemokine biology in the pathogenesis of bronchiolitis obliterans syndrome. *J Immunol*. 2002;169(2):1037-49.
34. Keane MP, Gomperts BN, Weigt S, Xue YY, Burdick MD, Nakamura H, et al. IL-13 is pivotal in the fibro-obliterative process of bronchiolitis obliterans syndrome. *J Immunol*. 2007;178(1):511-9.
35. Lama VN, Belperio JA, Christie JD, El-Chemaly S, Fishbein MC, Gelman AE, et al. Models of Lung Transplant Research: a consensus statement from the National Heart, Lung, and Blood Institute workshop. *JCI Insight*. 2017;2(9).
36. Belperio JA, Keane MP, Burdick MD, Gomperts BN, Xue YY, Hong K, et al. CXCR2/CXCR2 ligand biology during lung transplant ischemia-reperfusion injury. *J Immunol*. 2005;175(10):6931-9.

37. Hu Z, Lancaster JN, Sasiponganan C, and Ehrlich LI. CCR4 promotes medullary entry and thymocyte-dendritic cell interactions required for central tolerance. *J Exp Med*. 2015;212(11):1947-65.
38. Chang AL, Miska J, Wainwright DA, Dey M, Rivetta CV, Yu D, et al. CCL2 Produced by the Glioma Microenvironment Is Essential for the Recruitment of Regulatory T Cells and Myeloid-Derived Suppressor Cells. *Cancer research*. 2016;76(19):5671-82.
39. Gilet J, Chang Y, Chenivesse C, Legendre B, Vorng H, Duez C, et al. Role of CCL17 in the generation of cutaneous inflammatory reactions in Hu-PBMC-SCID mice grafted with human skin. *J Invest Dermatol*. 2009;129(4):879-90.
40. Larsen CP, Morris PJ, and Austyn JM. Migration of dendritic leukocytes from cardiac allografts into host spleens. A novel pathway for initiation of rejection. *J Exp Med*. 1990;171(1):307-14.
41. Lee I, Wang L, Wells AD, Dorf ME, Ozkaynak E, and Hancock WW. Recruitment of Foxp3+ T regulatory cells mediating allograft tolerance depends on the CCR4 chemokine receptor. *J Exp Med*. 2005;201(7):1037-44.
42. Ochando JC, Homma C, Yang Y, Hidalgo A, Garin A, Tacke F, et al. Alloantigen-presenting plasmacytoid dendritic cells mediate tolerance to vascularized grafts. *Nat Immunol*. 2006;7(6):652-62.
43. Miyajima M, Chase CM, Alessandrini A, Farkash EA, Della Pelle P, Benichou G, et al. Early acceptance of renal allografts in mice is dependent on foxp3(+) cells. *Am J Pathol*. 2011;178(4):1635-45.
44. Bueno V, and Pestana JO. The role of CD8+ T cells during allograft rejection. *Braz J Med Biol Res*. 2002;35(11):1247-58.
45. Kalish RS, and Askenase PW. Molecular mechanisms of CD8+ T cell-mediated delayed hypersensitivity: implications for allergies, asthma, and autoimmunity. *J Allergy Clin Immunol*. 1999;103(2 Pt 1):192-9.
46. Sachs DH, Kawai T, and Sykes M. Induction of tolerance through mixed chimerism. *Cold Spring Harb Perspect Med*. 2014;4(1):a015529.
47. Belperio JA, Lake K, Tazelaar H, Keane MP, Strieter RM, and Lynch JP, 3rd. Bronchiolitis obliterans syndrome complicating lung or heart-lung transplantation. *Semin Respir Crit Care Med*. 2003;24(5):499-530.
48. Weigt SS, Wang X, Palchevskiy V, Patel N, Derhovanessian A, Shino MY, et al. Gene Expression Profiling of Bronchoalveolar Lavage Cells During *Aspergillus* Colonization of the Lung Allograft. *Transplantation*. 2018;102(6):986-93.
49. Misslitz A, Bernhardt G, and Forster R. Trafficking on serpentines: molecular insight on how maturing T cells find their winding paths in the thymus. *Immunol Rev*. 2006;209:115-28.
50. Weninger W, and von Andrian UH. Chemokine regulation of naive T cell traffic in health and disease. *Semin Immunol*. 2003;15(5):257-70.
51. Guerder S, and Matzinger P. A fail-safe mechanism for maintaining self-tolerance. *J Exp Med*. 1992;176(2):553-64.
52. Belperio JA, Burdick MD, Keane MP, Xue YY, Lynch JP, 3rd, Daugherty BL, et al. The role of the CC chemokine, RANTES, in acute lung allograft rejection. *J Immunol*. 2000;165(1):461-72.
53. Buhler L, Alwayn IP, Appel JZ, 3rd, Robson SC, and Cooper DK. Anti-CD154 monoclonal antibody and thromboembolism. *Transplantation*. 2001;71(3):491.
54. Kawai T, Andrews D, Colvin RB, Sachs DH, and Cosimi AB. Thromboembolic complications after treatment with monoclonal antibody against CD40 ligand. *Nat Med*. 2000;6(2):114.
55. Okada T, and Cyster JG. CC chemokine receptor 7 contributes to Gi-dependent T cell motility in the lymph node. *J Immunol*. 2007;178(5):2973-8.
56. Webster KE, Walters S, Kohler RE, Mrkvan T, Boyman O, Surh CD, et al. In vivo expansion of T reg cells with IL-2-mAb complexes: induction of resistance to EAE and long-term acceptance of islet allografts without immunosuppression. *J Exp Med*. 2009;206(4):751-60.

57. Zhang N, Schroppel B, Lal G, Jakubzick C, Mao X, Chen D, et al. Regulatory T cells sequentially migrate from inflamed tissues to draining lymph nodes to suppress the alloimmune response. *Immunity*. 2009;30(3):458-69.
58. Huser N, Tertilt C, Gerauer K, Maier S, Traeger T, Assfalg V, et al. CCR4-deficient mice show prolonged graft survival in a chronic cardiac transplant rejection model. *Eur J Immunol*. 2005;35(1):128-38.
59. Ofek E, Sato M, Saito T, Wagnetz U, Roberts HC, Chaparro C, et al. Restrictive allograft syndrome post lung transplantation is characterized by pleuroparenchymal fibroelastosis. *Mod Pathol*. 2013;26(3):350-6.
60. Stewart S, Fishbein MC, Snell GI, Berry GJ, Boehler A, Burke MM, et al. Revision of the 1996 working formulation for the standardization of nomenclature in the diagnosis of lung rejection. *J Heart Lung Transplant*. 2007;26(12):1229-42.
61. Palchevskiy V, Hashemi N, Weigt SS, Xue YY, Derhovanessian A, Keane MP, et al. Immune response CC chemokines CCL2 and CCL5 are associated with pulmonary sarcoidosis. *Fibrogenesis Tissue Repair*. 2011;4:10.
62. Livak KJ, and Schmittgen TD. Analysis of relative gene expression data using real-time quantitative PCR and the 2(-Delta Delta C(T)) Method. *Methods*. 2001;25(4):402-8.
63. Korin YD, Lee C, Gjertson DW, Wilkinson AH, Pham TP, Danovitch GM, et al. A novel flow assay for the detection of cytokine secreting alloreactive T cells: application to immune monitoring. *Hum Immunol*. 2005;66(11):1110-24.
64. Lausch RN, Monteiro C, Kleinschrodt WR, and Oakes JE. Superiority of antibody versus delayed hypersensitivity in clearance of HSV-1 from eye. *Invest Ophthalmol Vis Sci*. 1987;28(3):565-70.

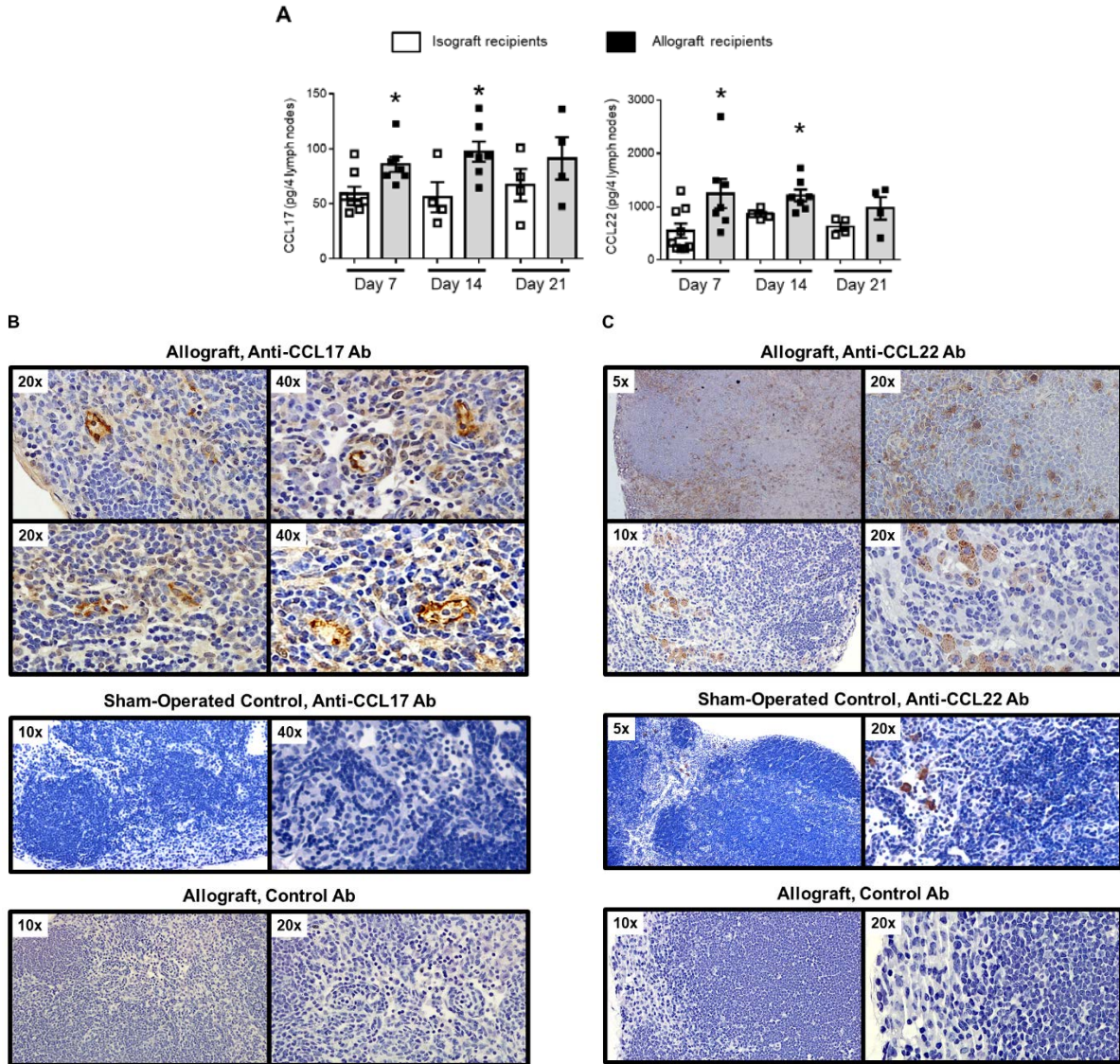


Figure 1. Draining allograft recipient lymph nodes have increased expression of CCL17 and CCL22. BALB/c airways were transplanted subcutaneously into C57BL/6 recipients (allografts), as compared to C57BL/6 airways transplanted into C57BL/6 recipients (isografts). Whole allograft draining nodes were harvested at days 7, 14, and 21 for protein analysis. (A) Bar graphs indicate the protein concentrations of CCL17 and CCL22 by Luminex from whole draining node homogenates from allograft and isograft recipients. (B) Representative immunohistochemical (IHC) staining for CCL17 and CCL22, as compared to appropriate control antibodies from allograft draining lymph nodes or sham operated CCR4^{+/+} mice lymph nodes at day 7. Allograft recipient CCL17 protein is expressed morphologically from HEV, as compared to virtually no staining in CCR4^{+/+} sham operated controls or for the control antibody. Allograft recipients CCL22 protein is detected morphologically on mononuclear phagocytes in the paracortical and subcapsular sinus, as compared to just a few mononuclear phagocytes only in the subcapsular sinus from the CCR4^{+/+} sham operated controls or virtually no staining for the control antibody. Protein data is representative of 4-9 mice per group. Error bars indicate SEM. Significance was determined by the Mann-Whitney test, * $p < 0.05$. IHC experiments involve (n=4) nodes from 4 different allograft recipients.

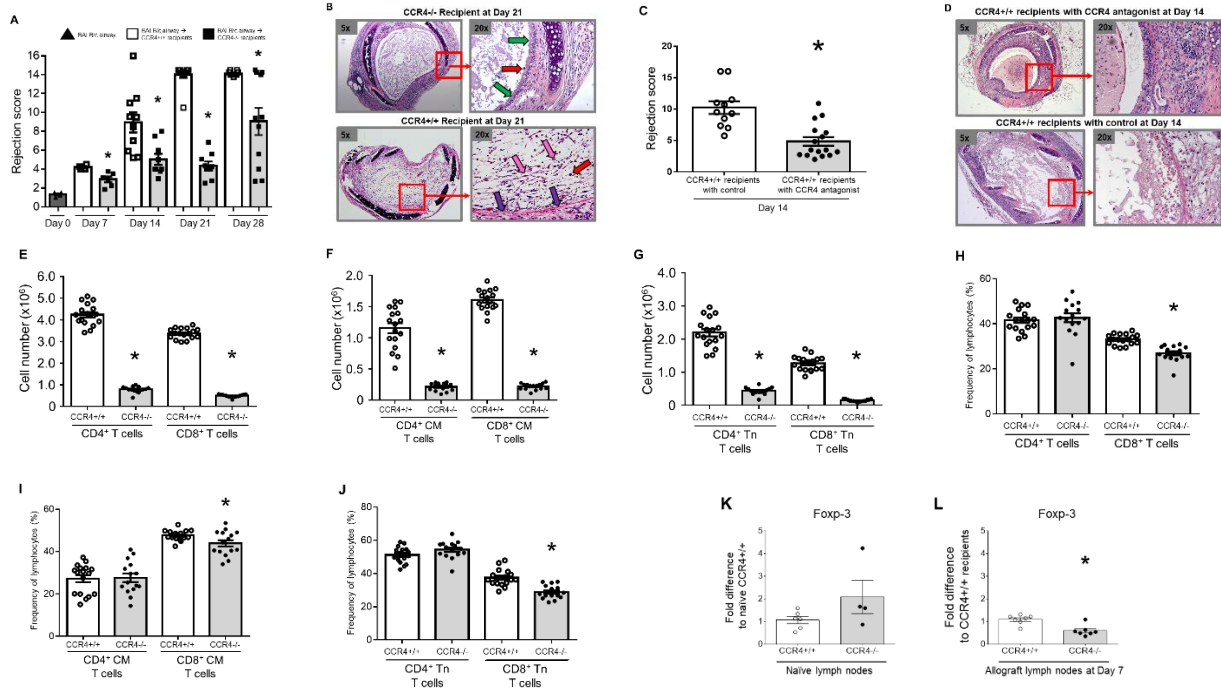


Figure 2. CCR4^{-/-} recipients of airway allografts attenuate rejection and have a reduction of T cells in their draining lymph nodes. BALB/c airways subcutaneously transplanted into CCR4^{-/-} and CCR4^{+/+} recipients and their allografts were analyzed for rejection scores while their whole draining lymph nodes were analyzed for T cell subpopulations via flow cytometry. **(A)** Bar graph indicates the rejection scores for donor BALB/c airways as well as allografts from either the CCR4^{-/-} or CCR4^{+/+} recipients at days 7, 14, 21 and 28. **(B)** Representative H&E staining of allografts from CCR4^{-/-} and CCR4^{+/+} recipients at day 21. CCR4^{-/-} recipients have limited intraluminal inflammation (red arrows), virtually normal epithelium (green arrows) and minimal matrix deposition without fibroblasts obstructing the lumen (i.e., fibro-obliteration). Section of the allograft is magnified to highlight the presence of a normal epithelial layer in the airway allografts from the CCR4^{-/-} recipients. Allografts from the CCR4^{+/+} recipients have a moderate amount of intraluminal inflammatory cells (red arrows), an absence of airway epithelial cells (purple arrows) and a presence of fibroblasts (pink arrows) causing fibro-obliteration of the lumen. See also Supplemental Figure 1. **(C)** Bar graph indicates the rejection scores of allografts from recipients treated with either the CCR4 antagonist or appropriate control at day 14. **(D)** Representative H&E staining of allografts from the CCR4 antagonist and control at day 14. Recipients with the CCR4 antagonist have a virtually normal epithelium and minimal matrix deposition without fibro-obliteration. Section of the allograft is magnified to show the presence of a normal epithelial layer in the airway allografts from the recipients treated with the CCR4 antagonist. Allografts from the control treated recipients have an absence of airway epithelial cells. **(E-J)** Bar graphs indicate the total number and frequency of CD4⁺ and CD8⁺ T cells and their naïve (Tn) and central memory (CM) T cell subpopulations from CCR4^{+/+} and CCR4^{-/-} allograft recipient lymph nodes at day 7. See also Supplemental Figure 2. **(K)** Bar graph indicates the lymph node expression of Foxp-3 by qPCR for naïve non-transplanted CCR4^{+/+} and CCR4^{-/-} mice nodes as well as **(L)** CCR4^{+/+} and CCR4^{-/-} allograft recipient nodes at day 7. Data is representative of 4-15 mice per group. Error bars indicate SEM. Significance was determined by Mann-Whitney or unpaired t test where appropriate, *p<0.05.

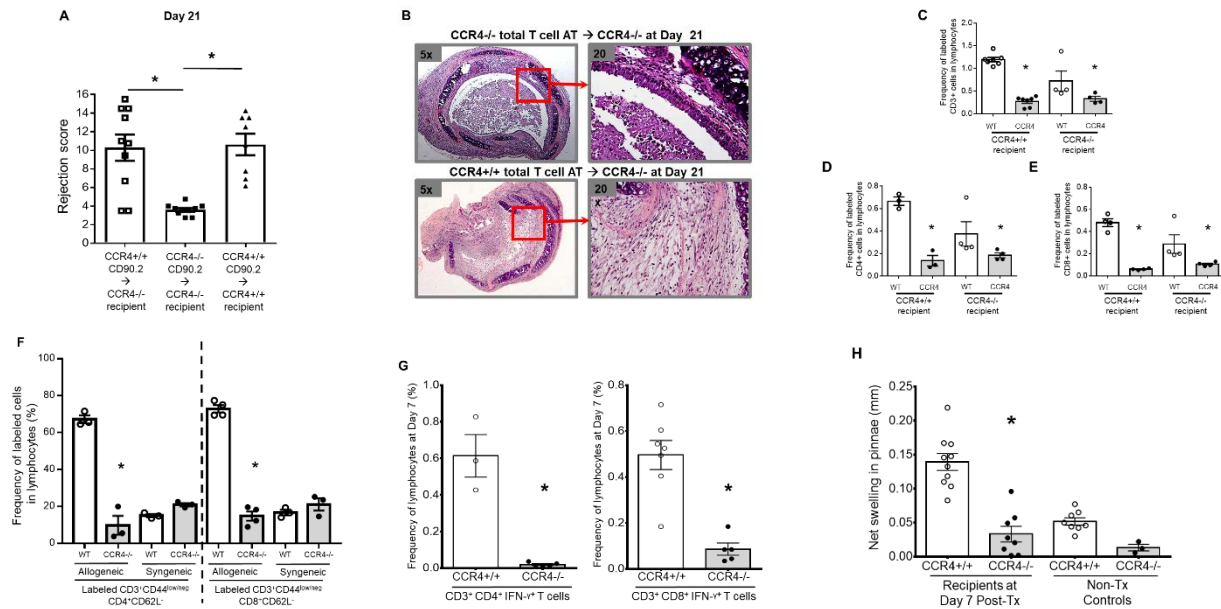


Figure 3. CCR4 expression is involved in naïve T cell (Tn) homing and intranodal activation. CD90.2 (1×10^7) T cells from either CCR4^{-/-} or CCR4^{+/+} naïve mice were transferred to either CCR4^{-/-} or CCR4^{+/+} recipients on day 0 and the allografts were analyzed for rejection scores at day 21. **(A)** Bar graph indicates the rejection scores. **(B)** Representative H&E staining showing that the transfer of CCR4^{+/+} T cells to CCR4^{-/-} recipients leads to severe rejection with a denuded epithelium and fibro-obliteration. However, the transfer of CCR4^{-/-} T cells to CCR4^{-/-} recipients has no significant epithelial injury or fibro-obliteration. In separate experiments, CFSE labeled T cells from CCR4^{+/+} (4.0uM, 5×10^6) and CCR4^{-/-} (0.25uM, 5×10^6) naïve mice were transferred at a 1:1 ratio into day 7 CCR4^{+/+} and CCR4^{-/-} allograft recipients or isograft (C57BL/6 airways to C57BL/6 recipients), and 18-hours later the draining nodes were analyzed for the frequency of labeled T cells as well as their activation based on CD62L shedding using flow cytometry. **(C-E)** Bar graphs depict the frequency of labeled CCR4^{-/-} and CCR4^{+/+} CD3⁺, CD4⁺ and CD8⁺ T cells. See also Supplemental Figure 3. **(F)** Bar graph depicts the frequency of labeled CD4⁺ and CD8⁺ T cells from CCR4^{-/-} and CCR4^{+/+} naïve mice that entered the lymph nodes and lose CD62L expression. See also Supplemental Figure 3. **(G)** Day 7 CCR4^{-/-} and CCR4^{+/+} allograft recipients draining lymph node cells (1×10^6) were challenged with (2×10^6) irradiated-BALB/c splenocytes and 16-hours later analyzed for alloresponsive CD4⁺ and CD8⁺ T cells via IFN- γ secretion. See also Supplemental Figure 4. **(H)** Day 7 CCR4^{-/-} and CCR4^{+/+} allograft recipients were challenges with (7.5×10^6) irradiated-BALB/c splenocytes with an intra-dermal injection into the pinna and analyzed for DTH response at 48-hours. Data is representative of 3-12 mice per group. Error bars indicate SEM. Significance was determined by Mann-Whitney, unpaired t test, or Kruskal-Wallis with post-hoc Dunn where appropriate, * $p < 0.05$.

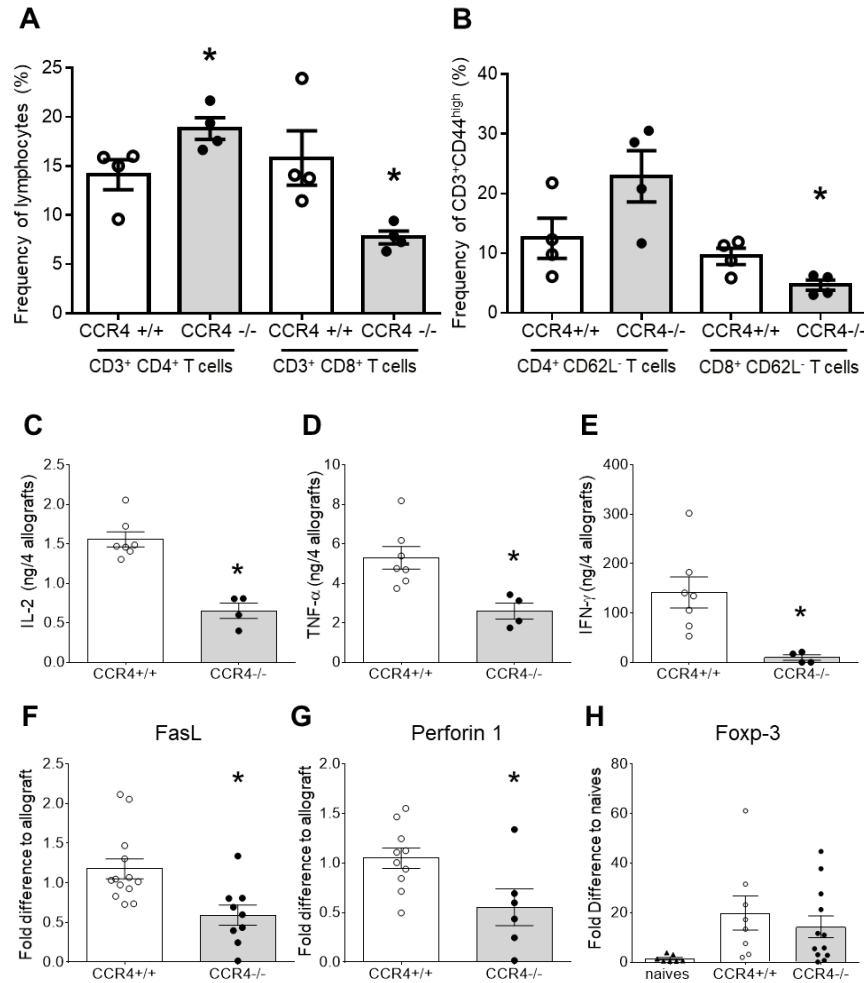


Figure 4. CCR4^{-/-} recipients have a reduction in airway allograft infiltrating cytotoxic lymphocytes and their mediators. Day 7 whole airway allografts from CCR4^{-/-} and CCR4^{+/+} recipients were analyzed for allograft infiltrating T cell subpopulations and cytotoxic mediators using flow cytometry, luminex and qPCR. **(A-B)** Bar graphs depict the frequency of allograft infiltrating, CD4⁺ and CD8⁺ T cells as well as their subpopulations. **(C-E)** Bar graphs depict the whole allograft homogenates protein concentrations for IL-2, TNF- α , and IFN- γ . **(F-H)** Bar graphs represent the whole allograft homogenates mRNA expression for FasL, perforin-1 and Foxp-3. Data is representative of 4-7 mice per group. Error bars indicate SEM. Significance was determined by Mann-Whitney, *p<0.05.

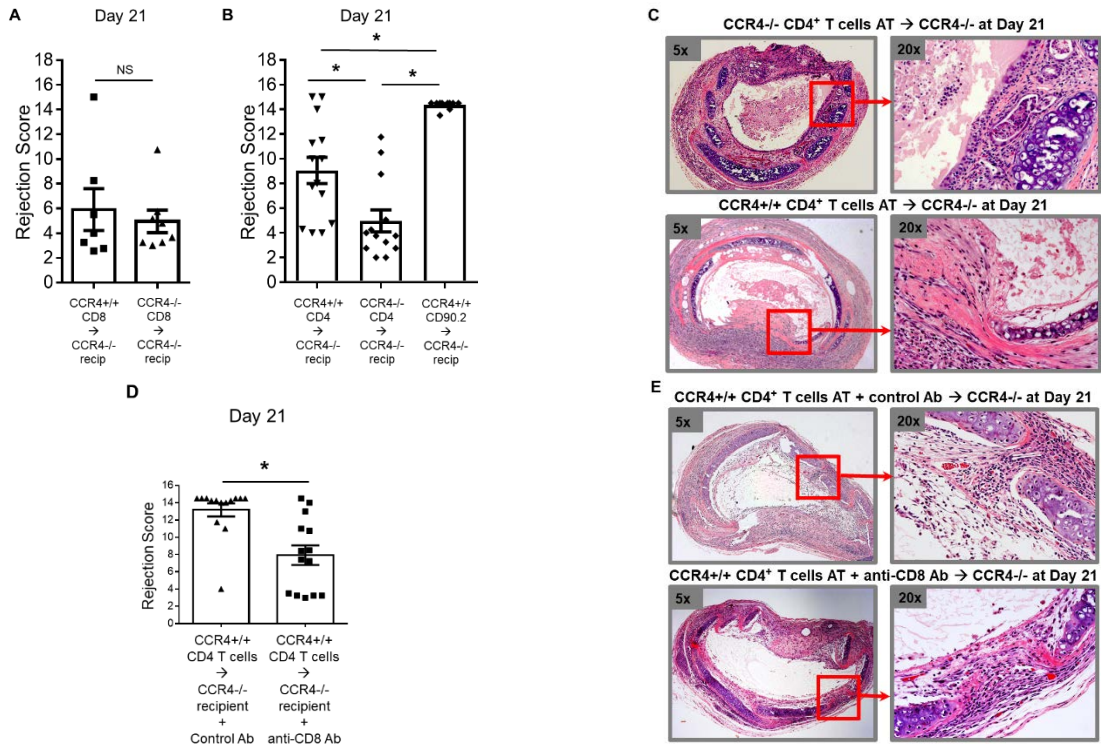


Figure 5. The hierarchy for T cells re-establishing rejection in the CCR4^{-/-} recipient mice. CD8⁺ (5×10^6), CD4⁺ (5×10^6) and CD90.2⁺ (1×10^7) T cells from either CCR4^{-/-} or CCR4^{+/+} naïve mice were transferred to CCR4^{-/-} recipients of BALB/c airway grafts on day 0 and the allografts were analyzed for rejection scores at day 21. Bar graph indicates the rejection scores of allografts from CCR4^{-/-} recipients with the transfer of (A) CD8 T cells and (B) CD4 and CD90.2 T cells. See also Supplemental Figure 5. (C) Representative H&E staining of day 21 transplanted BALB/c airways from adoptively transferred CD4⁺ T cells from either CCR4^{+/+} or CCR4^{-/-} naïve mice transferred into CCR4^{-/-} recipients at day 0. CCR4^{-/-} recipients with transferred CCR4^{-/-} CD4⁺ T cells have a virtually normal epithelium without fibroblasts obstructing the lumen. Allografts from the CCR4^{-/-} recipients with transferred CCR4^{+/+} CD4⁺ T cells have a denuded airway epithelium with a moderate amount of fibroblasts invading the airway lumen. In separate experiments, CCR4^{+/+} CD4⁺ T cells (5×10^6) were transferred to CCR4^{-/-} recipients with either control Ab or the depleting anti-CD8 Ab delivered at days -1, 7 and 14, and the allografts were analyzed for rejection scores at day 21. (D) Bar graph depicts the rejection scores of allografts from CCR4^{-/-} recipients with the transfer of CCR4^{+/+} CD4⁺ T cells with or without anti-CD8 Ab. (E) CCR4^{-/-} recipients with transferred CCR4^{+/+} CD4⁺ T cells plus a control Ab have a loss of airway epithelium with a moderate amount of fibroblasts obstructing the lumen. CCR4^{-/-} recipients with transferred CCR4^{+/+} CD4⁺ T cells plus an anti-CD8 Ab have a denuded airway epithelium and minimal airway invading fibroblasts. Data is representative of 10-16 mice per group. Error bars indicate SEM. Significance was determined by Mann-Whitney or Kruskal-Wallis with post-hoc Dunn where appropriate. * $p < 0.05$.

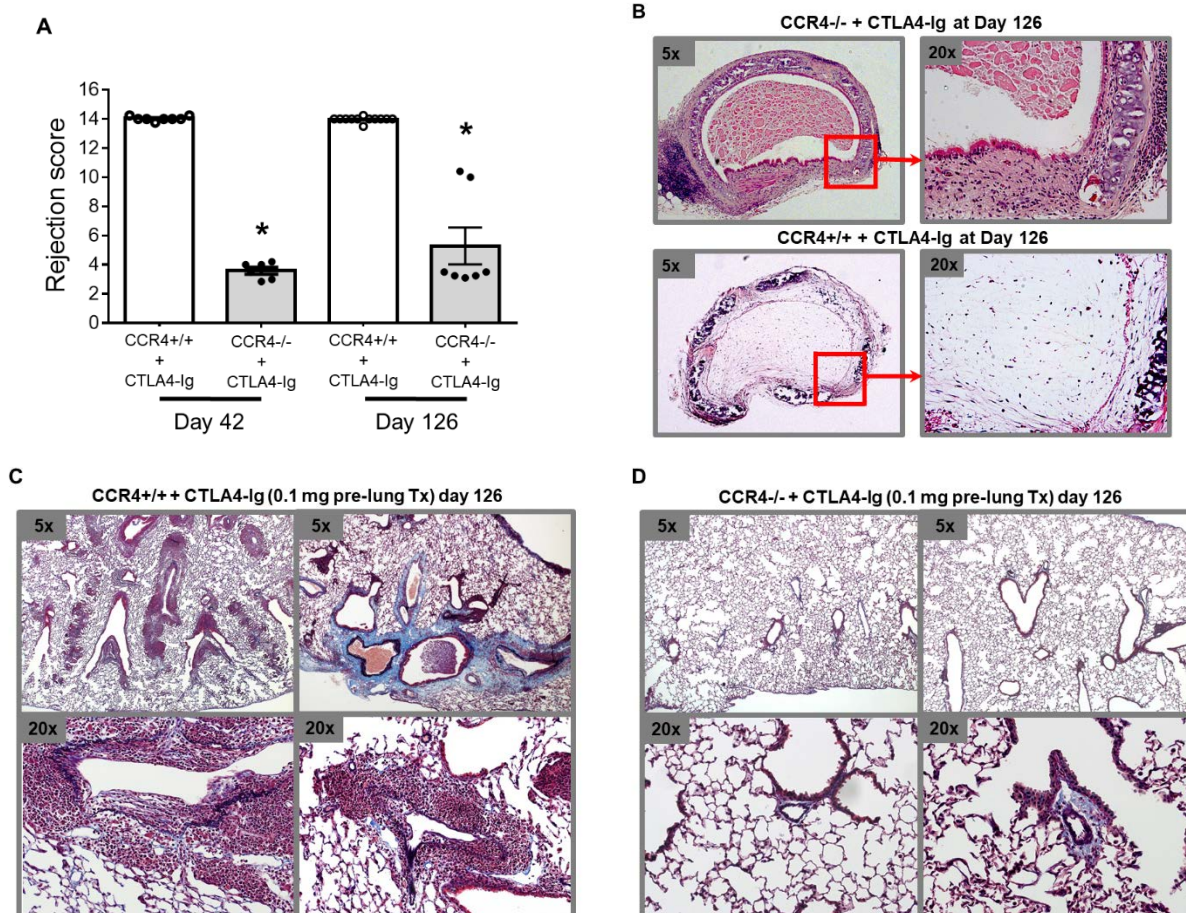


Figure 6. CTLA4-Ig combined with CCR4^{-/-} recipients leads to long-term allograft accommodation in two models of allograft rejection. CTLA4-Ig given intraperitoneal (i.p.) at 0.2 mg on day 0 prior to airway transplantation and at days 2, 4, and 6 post-transplant to CCR4^{-/-}, as compared to CCR4^{+/+} recipients were evaluated for rejection. (A) Bar graph indicates the rejection scores for CTLA4-Ig treated CCR4^{-/-} and CCR4^{+/+} allograft recipients at days 42 and 126. See also Supplemental Figure 6. (B) Day 126 representative H&E staining of airway allografts from CCR4^{-/-} and CCR4^{+/+} recipients given CTLA4-Ig. CTLA4-Ig given to CCR4^{-/-} recipients demonstrate virtually normal airways with intact ciliated epithelium and no fibro-obliteration. CTLA4-Ig given to CCR4^{+/+} recipients leads to airways that are rejected, without epithelium, and invaded by fibroblasts causing fibro-obliteration. Section of airway allograft is magnified to show the presence of the epithelial layer in CTLA4-Ig + CCR4^{-/-} and absence of the epithelial layer with fibro-obliteration in the CTLA4-Ig + CCR4^{+/+} recipients. Orthotopic single lung transplant to CCR4^{-/-} and CCR4^{+/+} recipients given CTLA4-Ig i.p. (0.1 mg) at day 0 just prior to transplant. (C) Day 126 representative elastin trichrome stain shows that CTLA4-Ig given to CCR4^{+/+} allograft recipients leads to high grade vascular, airway and pleural rejection with fibrosis. (D) Day 126 representative elastin trichrome stain shows that CTLA4-Ig given to CCR4^{-/-} allograft recipients leads to virtually normal lung allografts. Data is representative of 4-12 mice per group. Error bars indicate SEM. Significance was determined by Mann-Whitney, *p<0.05.